The influence of sediment sources on radium-derived estimates of Submarine Groundwater Discharge

Valentí Rodellas[1]*, Jordi Garcia-Orellana[1], Pere Masqué[1,2,3], Joan S. Font-Muñoz[4]

[1] Institut de Ciència i Tecnologia Ambientals & Departament de Física. Universitat Autònoma de Barcelona, E-08193 Bellaterra, Catalonia, Spain

[2] The University of Western Australia Oceans Institute, University of Western Australia, 35 Stirling Highway, Crawley 6009, Australia

[3] School of Natural Sciences, Centre for Marine Ecosystems Research, Edith Cowan University, Joondalup WA 6027, Australia

[4] Institut Mediterrani d'Estudis Avançats, IMEDEA (UIB-CSIC), Esporles, Mallorca, Spain

* Corresponding author: valenti.rodellas@uab.cat. (+34) 93 581 11 91.
Facultat de Ciències (C3-348). Campus UAB.
E-08193 Bellaterra, Catalonia, Spain

ABSTRACT

The influence of sediments on the determination of SGD by using Ra isotopes was investigated in the Port of Maó (Balearic Islands, NW Mediterranean). This natural harbor was selected because SGD occurs all along its southern boundary and it is covered by fine-grained sediments that are frequently resuspended due to vessel maneuvering. Comprehensive seasonal Ra mass balances were constructed for the waters of the Port of Maó using both short- (^{224}Ra) and long- (^{228}Ra) lived Ra isotopes. SGD flows to the Port of Maó obtained by using ^{228}Ra revealed a seasonal pattern, likely dominated by the recharge cycle, with maximum SGD rates during the wet seasons ((180 ± 100)·10^{3} m^{3}·d^{-1} in fall) and minimum flows during summer ((56 ± 35)·10^{3} m^{3}·d^{-1}). The results also showed that the Ra flux from bottom sediments, through diffusion and due to releases associated to resuspension events, represented a significant source of Ra to the harbor waters. This sedimentary source accounted for a major fraction of the ^{224}Ra supplied to the system (30 - 90%, depending on the season), whereas the sediment influence on the ^{228}Ra mass balance was significantly lower (10 - 40%) due to its slower production rate. These findings suggested that attributing Ra inputs to the water column solely to SGD in systems covered by fine-grained sediments and/or affected by processes that favor Ra exchange across the sediment-water interface might not be accurate, requiring a detailed evaluation of the sediment sources. The inputs from sediments are often difficult to quantify, but using long-lived Ra isotopes to estimate the SGD flow may minimize the effect of a poor characterization of the sediment source.

KEYWORDS: Radium isotopes, Submarine Groundwater Discharge, Sediments, Mediterranean Sea

49 **GRAPHICAL ABSTRACT**

50

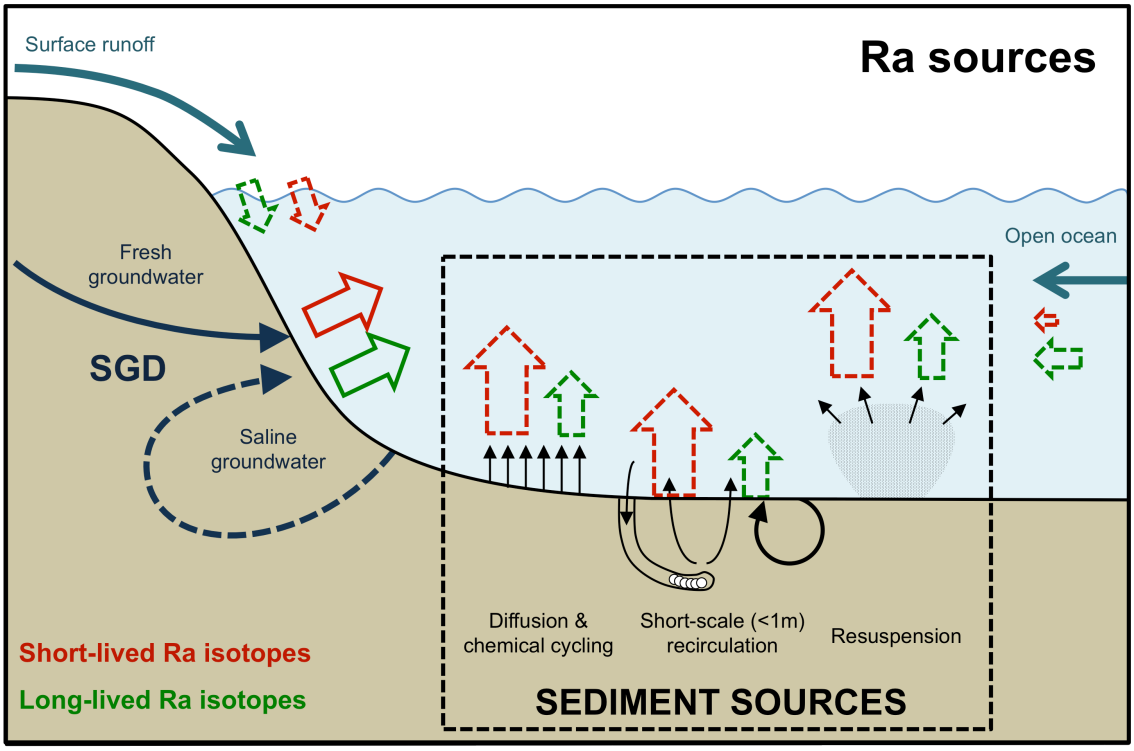

51
52

1. INTRODUCTION

Submarine Groundwater Discharge (SGD) is the flow of water through continental margins from the seabed to the coastal ocean, with scale lengths of meters to kilometers, which is composed of fresh meteoric groundwater and former seawater recirculating through permeable sediments (Burnett et al., 2003; Moore, 2010). Some studies have shown that SGD is a relevant source of terrestrial compounds to the coastal ocean, including nutrients (Slomp and Van Cappellen, 2004), trace metals (Windom et al., 2006), dissolved inorganic carbon (Cai et al., 2003) or natural radionuclides (Garcia-Orellana et al., 2013). The magnitude of SGD into coastal waters is commonly determined by using natural tracers, such as the naturally occurring Ra isotopes (^{224}Ra ($T_{1/2}$ = 3.66 d), ^{223}Ra ($T_{1/2}$ = 11.4 d), ^{228}Ra ($T_{1/2}$ = 5.75 y) and ^{226}Ra ($T_{1/2}$ = 1600 y)). Ra isotopes have been successfully used as tracers of SGD in a wide variety of systems, mainly because they behave conservatively in seawater, they are highly enriched in SGD relative to coastal seawater and their half-lives vary in a wide range, allowing tracing processes at different time-scales and quantifying multiple sources of SGD (e.g. Charette et al., 2001; Moore et al., 2008; Rama and Moore, 1996). All the approaches used to estimate SGD by using Ra isotopes depend on the evaluation of the Ra flux supplied by SGD, which requires accurately constraining all the Ra sources other than SGD (e.g. releases from sediments, riverine discharge).

Seafloor sediments may be a continuous source of Ra isotopes to the water column through diffusion, erosion or resuspension, but also through short-scale recirculation processes (mm to cm), such as topography-induced advection, wave pumping, ripple migration, shear or bioirrigation (Breier et al., 2009; Garcia-Orellana et al., 2014;

78 Rama and Moore, 1996; Santos et al., 2012). Most studies involving Ra isotopes as
79 tracers of SGD have shown that inputs of Ra from seafloor sediments are often small
80 in relation to the SGD source term (Beck et al., 2007; Charette et al., 2003; Garcia-
81 Solsona et al., 2008b; Rama and Moore, 1996; Rodellas et al., 2012). Conversely,
82 recent studies in shallow embayments with fine-grained sediments and/or affected
83 by processes that favor Ra exchange across the sediment-water interface (e.g.
84 bioirrigation, resuspension, hypoxia) have demonstrated that the sedimentary source
85 can supply a relevant flux of Ra isotopes, which may be comparable to SGD-derived
86 Ra inputs (Breier et al., 2010, 2009; Colbert and Hammond, 2008; Garcia-Orellana et
87 al., 2014; Gleeson et al., 2013). The relevance of the sedimentary source may be
88 particularly important for short-lived Ra isotopes (^{223}Ra and ^{224}Ra), since their fast
89 regeneration time within the surficial sediments allows its almost-continuous release
90 to the water column. Therefore, attributing Ra inputs to the water column solely to
91 SGD may not always be well justified, requiring a detailed evaluation of the
92 sedimentary source.
93
94 The natural harbor of Maó (Minorca, Balearic Islands, NW Mediterranean) is an ideal
95 setting to assess the potential contribution of sediments on a Ra mass balance to
96 estimate SGD, since: i) there are evidences of fresh groundwater inflowing along its
97 southern shore; and ii) it is covered by fine-grained sediments that are subjected to
98 frequent resuspension events provoked by maritime traffic of deep draft vessels
99 (Garcia-Orellana et al., 2011), potentially representing a relevant mechanism to
100 introduce Ra isotopes to the water column. We constructed seasonal comprehensive
101 Ra mass balances for the waters of the Port of Maó, using both short- and long-lived

Ra isotopes (^{224}Ra and ^{228}Ra, respectively), considering the differences among Ra isotopes and the potential seasonal variability of the Ra sources.

2. METHODS

2.1. Field site

The Port of Maó (Fig. 1) is a semi-enclosed embayment with restricted exchange with the open sea, as a consequence of its elongated shape (5 km length and a maximum width of 0.8 km) and its shallow mouth (13 m). Indeed, the whole harbor is a shallow water body with depths lower than 10 m in the inner part and a maximum water column depth of 29 m in the central part of the harbor.

The Port of Maó is located in the middle of a fault that divides the island in two geomorphological settings: an impermeable northern sector of Mesozoic rocks and a broad permeable Miocene limestone platform that constitutes the main aquifer to the south (Fornós et al., 2004). This aquifer, named Migjorn, supplies most of the total extracted water from the island ($\sim 11 \cdot 10^6$ m^3 yr^{-1}), mainly for tourism and agriculture purposes (Garcia-Solsona et al., 2010a). The aquifer permeability increases towards the coastline as a consequence of a major karstic development that results in direct or diffuse groundwater discharge to the sea (Fayas, 1972). Due to this hydrogeological division, most of the groundwater inputs into the harbor are located on the southern shoreline. Indeed, several natural wells and springs exist along the southern area of the harbor, and groundwater springs inflowing directly to the harbor can be visually identified. Aside from groundwater discharge, freshwater inputs are restricted to the discharge of a small stream in the inner harbor, named Torrent des Gorg, and runoff from eventual precipitation events from the northern shore and the towns of Maó and Es Castell. The average annual rainfall is about 600 mm, with dry summers and maxima in spring and autumn.

The Port of Maó has been subjected to continuous urban and industrial dumps from the city of Maó and the industries settled around the harbor. This has led, for instance, to a progressive contamination of seafloor sediments with metals (Ag, Cd, Cu, Ni, Pb, among others; Garcia-Orellana et al., 2011). It is also an important touristic destination, and cruises and large vessels frequently circulate along the harbor, especially during the summer season. Since most of these vessels have drafts between 6 to 9 m and given the shallowness of the harbor (the transit channel is 10-14 m deep), propellers of large vessels frequently resuspend significant amounts of sediments, particularly when maneuvering to dock, favoring the release of contaminants from the sediments to the water column (Garcia-Orellana et al., 2011).

2.2. Sample collection

Four seasonal surveys (July 2010, October 2010, March 2011 and June 2011) were conducted at the Port of Maó. 15 stations distributed along the harbor were sampled during each survey (Fig. 1). Depth profiles of temperature and salinity were measured at each station with a CTD (SBE-25, Seabird Electronics). Water samples for Ra isotopes were collected from 1 m depth (surface) at each station, and also at 10 and 20 m at station 19 in October 2010, March 2011 and June 2011. Samples for Ra analysis were stored in 60 L containers.

Groundwater was sampled for Ra isotopes, salinity and temperature measurements from 8 coastal wells distributed along the southern shoreline and two small islands within the harbor and from the small stream inflowing to the inner harbor (Fig. 1). Whereas on July 2010 and October 2010 the stream was sampled in the freshwater area, on March 2011 and June 2011 the samples were collected from the estuarine

zone. Finally, one sediment core was also collected at the inner harbor to determine the diffusive fluxes of Ra isotopes from seafloor sediments to the harbor waters (Fig. 1).

In addition to the seasonal samplings, a 3-day intensive monitoring was conducted between 8 and 10 May 2012 to evaluate the relevance of sediment resuspension provoked by vessels maneuvering to dock as a source of Ra isotopes to the water column. Two resuspension events occurred during the studied period, driven by the same deep-draught vessel (draught = 6 m) that docked in the harbor the 1st and the 3rd day of the monitoring period. During this 3-day survey, a station located in the inner harbor (Fig. 1) was sampled 14 times, collecting 2 filtered samples for Ra isotopes each time to characterize surface (1 m depth) and (7 m depth) deep waters. Depth profiles of suspended particles were measured during the first two days at each sampling time by using laser in situ scattering and transmissometry (LISST-100X, Sequoia Scientific). This instrument obtains the particle volume concentration ($\mu L \cdot L^{-1}$) by laser diffraction (Agrawal and Pottsmith, 2000).

2.3. Analytical methods

The water samples were filtered through columns loaded with MnO_2-impregnated acrylic fiber (hereafter Mn-fibers) at a flow rate <1 $L \cdot min^{-1}$ to quantitatively extract the Ra isotopes (Moore and Reid, 1973). Acrylic fiber without MnO_2 was used as a pre-filter to extract water particles. In the laboratory, Mn-fibers were rinsed with radium-free deionized water, partially dried (Sun and Torgersen, 1998), and placed in a Radium Delay Coincidence Counter (RaDeCC) to quantify the short-lived radium isotopes (^{223}Ra and ^{224}Ra, as well as ^{228}Th to estimate the ^{224}Ra excess not supported by its parent) (Moore and Arnold, 1996)). Uncertainties were estimated according to (Garcia-Solsona et al., 2008a). Then, the Mn-fibers were ashed (820 ºC, 16 h), ground and transferred to counting vials to determine the long-lived Ra isotopes (^{226}Ra and ^{228}Ra) by gamma spectrometry using a high-purity well-type Ge detector. Measurements were carried out after aging the samples for a minimum of 3 weeks to ensure the equilibrium between ^{226}Ra and its daughters. ^{226}Ra and ^{228}Ra were determined through the ^{214}Pb and ^{228}Ac photopeaks at 352 keV and 911 keV, respectively. All Ra activities were corrected for radioactive decay to the sampling time.

Ra fluxes diffused from sediments were estimated from the incubation of the sediment core collected at the inner harbor, following the methodology described by (Rodellas et al., 2012). Briefly, once at the laboratory, the overlying water of the sediment core was replaced with Ra-free seawater. The seawater added to the incubation core was continuously circulated through a Mn-fiber to extract the Ra isotopes and bring the Ra-free water back to the incubation chamber. The fiber was removed to determine its content on Ra isotopes and replaced by a new one after

each incubation period (12, 24, 36, 48, 72 and 96 hours). The Ra diffusive fluxes were determined by averaging the decay corrected Ra activity divided by each incubation time and referenced to the core surface area (0.05 m^2).

198 **3. RESULTS**

199 **3.1. Seasonal sampling**

200 Salinity distributions along the harbor showed marked differences among the 4
201 surveys, likely reflecting seasonal variations on freshwater inputs (Fig. 2). During
202 October 2010, a salinity gradient was observed along the Port of Maó, with lower
203 salinities in the inner harbor and increasing salinities towards the harbor outlet.
204 Contrarily, a strong vertical stratification was observed in March 2011, without a
205 clear gradient along the harbor, likely suggesting the presence of freshwater inputs
206 and a rapid horizontal mixing. During summer, minor freshwater inputs,
207 characteristic of the dry season, were revealed by salinities measured at the inner
208 harbor being similar (June 2011) or even higher (July 2010) than those measured in
209 the open sea, likely reflecting minor freshwater inputs and/or an intense evaporation
210 of harbor waters.

211

212 The data on the concentrations of Ra isotopes for the four samplings campaigns is
213 presented in Fig. 3. An enrichment in the concentrations of ^{223}Ra, ^{224}Ra and ^{228}Ra was
214 observed in surface waters from the inner harbor relative to samples offshore, with a
215 decreasing trend towards the harbor outlet, suggesting that most of Ra inputs occur
216 at the inner harbor and/or there is a major dilution with open sea water at external
217 stations (Table 1). Stronger horizontal gradients along the harbor were observed for
218 short-lived Ra isotopes, and, to a lesser extent, for ^{228}Ra (Fig. 3). ^{226}Ra presented
219 relatively homogeneous concentrations along the harbor in all the sampling surveys,
220 comparable to those measured at the offshore station, revealing a lack of major ^{226}Ra
221 inputs (Table 1; Fig. 3). Concentration gradients for ^{223}Ra, ^{224}Ra and ^{228}Ra along the
222 harbor were smoothed in March 2011, likely as a consequence of a rapid horizontal

223 homogenization of surface waters, as indicated by the surface salinity distribution
224 (Fig. 2). Concentrations of long-lived Ra isotopes were relatively constant along the
225 water column for all the seasons and regardless variations on salinity, as derived
226 from the depth profile conducted at station #19 in October 2010, March 2011 and
227 June 2011. However, concentrations of short-lived Ra isotopes showed a significant
228 decrease with depth in October 2010 and March 2011. Since this decrease is only
229 observed for short-lived Ra isotopes, it is likely caused by radioactive decay, because
230 mixing with open seawater would also reduce the concentrations of long-lived Ra
231 isotopes (^{224}Ra and ^{228}Ra profiles shown in Table 2).
232
233 **3.2. Characterization of groundwater and stream water**
234 Most of the groundwater samples collected from wells and springs located close to
235 the harbor shoreline (less than 50 m) presented salinities ranging from 0.7 to 1.6,
236 suggesting minimal seawater intrusion. Only the wells located in small islands (W5
237 and W7) revealed an exchange with the sea (salinities of 8.9 and 12.6, respectively)
238 (Table 3).
239
240 The concentrations of Ra measured in the coastal wells showed minimal seasonal
241 variations (e.g. ^{228}Ra concentrations measured in W8 were 199 ± 11, 229 ± 10 and
242 228 ± 5 dpm·100L^{-1} in October 2010, March 2011 and June 2011, respectively). Given
243 the minimal seasonal variation, concentrations of all the samples from the same well
244 were averaged to obtain a single estimate for each site (Table 3).
245
246 Groundwater samples were enriched in all the Ra isotopes relative to seawater (Table
247 3). In general, ^{228}Ra concentrations in groundwater were higher than concentrations

of ^{224}Ra and ^{226}Ra for most of the collected samples (median activity ratios (AR): $^{224}Ra/^{228}Ra$ = 0.65; $^{228}Ra/^{226}Ra$ = 2.0). These differences among Ra isotopes in groundwater are likely explained by two major factors: i) the $^{228}Ra/^{226}Ra$ AR in groundwater is reflecting the parental Th/U ratio in the carbonate host rocks (Garcia-Solsona et al., 2010a; Moore, 2003); and ii) most of the sampled wells have large dimensions and nowadays are not frequently used, likely resulting in stagnant groundwater in the wells for long periods leading to the partial decay of short-lived Ra isotopes with respect to the long-lived ones.

Concentrations of Ra isotopes measured in the stream inflowing to the inner part of the harbor are also presented in Table 3. Ra concentrations measured in both the freshwater (salinity of 0.9) and the estuarine areas (salinity of 11.2) were comparable to those measured in the inner harbor.

3.3. Three-day intensive monitoring

The passing and maneuvering of vessels during the three-day sampling in May 2012 induced the resuspension of significant amounts of seafloor sediments, which could be visually observed (Fig. 4), enhancing the concentration of suspended particles (from <0.3 $\mu L \cdot L^{-1}$ to >1 $\mu L \cdot L^{-1}$) in the entire water column of the inner harbor (Fig. 5). After the vessel-driven resuspension events, concentrations of short-lived Ra isotopes in both surface and deep waters increased significantly, particularly after the 2nd vessel docking (1st docking: increases of 50 and 30% with respect to the ^{223}Ra and ^{224}Ra concentrations before the resuspension event, respectively; 2nd docking: concentration increases of 80 and 100% for ^{223}Ra and ^{224}Ra, respectively) (Fig. 6). Unlike short-lived Ra isotopes, concentrations of ^{226}Ra and ^{228}Ra did not increase

substantially (less than 20%) as a consequence of the sediment resuspension events (Fig. 6). This reduced increase on the concentrations of long-lived Ra isotopes is likely related to their long regeneration time, that results in minimum amounts of long-lived Ra isotopes available for desorption when sediment resuspension events occur.

3.4. Diffusive sediment fluxes

The diffusive fluxes of Ra isotopes from sediments obtained from the incubation experiment were 4.9 ± 1.1, 110 ± 15, 11.3 ± 2.4 and 11.7 ± 0.8 dpm·d^{-1}·m^{-2} for ^{223}Ra, ^{224}Ra, ^{226}Ra and ^{228}Ra, respectively. Differences among fluxes from different Ra isotopes are related to the abundance in sediments, the regeneration time of each isotope, which is set by their respective decay constants, and the relative recoil rates. These fluxes are mainly reflecting molecular diffusion and represent an upper estimate, since the continuous replacement of overlying waters with Ra-free water maximizes the gradient between pore and overlying waters (Beck et al., 2007; Rodellas et al., 2012). Fluxes are comparable to those obtained in previous studies in muddy sediments from coastal Mediterranean environments (Garcia-Solsona et al., 2008b) and throughout the world (Beck et al., 2007; Garcia-Orellana et al., 2014; Moore et al., 2008).

4. DISCUSSION

4.1. Ra mass balance

Several approaches have been used to estimate SGD into coastal areas by using Ra isotopes, including end-member mixing models (e.g. Charette et al. 2013), determining Ra fluxes offshore from eddy diffusive mixing (e.g. Dulaiova et al. 2006), or developing Ra mass balances (e.g. Beck et al. 2007). The use of a comprehensive Ra mass balance is likely the most appropriate method to assess the magnitude of SGD in coastal systems with several potential Ra sources, since the other approaches generally assume that SGD is the dominant Ra input. The Ra mass balance relies on the assumption that the Ra concentrations in the harbor are in steady state during a given period, and thus Ra isotopes must be continuously supplied to balance their outputs. By constraining all the potential Ra inputs and outputs, the Ra flux supplied by SGD can be evaluated by difference.

In the case of the Port of Maó, we identified several potential Ra inputs, including diffusion from sediments (J_{diff}), desorption from resuspended sediments (J_{des}), the stream water discharge (J_{str}) and SGD (J_{SGD}). Losses of Ra from the system would occur by radioactive decay (J_{λ}) and net export to the coastal sea (J_{sea}). Biological uptake, in situ production from dissolved Th parents and atmospheric inputs are negligible relative to the other source or removal terms (Charette et al., 2008). Thus, the mass balance for Ra isotopes can be expressed as follows:

$$J_{\lambda}+J_{sea} = J_{diff} + J_{des} + J_{str} + J_{SGD} \quad (1)$$

315 where sinks and sources of Ra are on the left- and right- hand sides of the equation,
316 respectively. For the purpose of this study, we focus on a short-lived Ra isotope
317 (^{224}Ra) and on a long-lived one (^{228}Ra). We have excluded ^{223}Ra, which would provide
318 equivalent information to that obtained from ^{224}Ra but with larger uncertainties, and
319 ^{226}Ra, because it is not significantly enriched in the harbor relative to open sea
320 waters, revealing that there are no relevant sources of this isotope in the harbor.
321
322 *Ra decay*
323 The decay term of the Ra mass balance can be obtained by multiplying the total Ra
324 inventory in harbor waters by the decay constants of ^{224}Ra (λ = 0.189 d^{-1}) and ^{228}Ra (λ
325 = $0.330 \cdot 10^{-3}$ d^{-1}). Total Ra inventories in the harbor are derived from the area-
326 weighted average Ra inventories from each station and the area of the study site
327 ($3.0 \cdot 10^{6}$ m^2). For each station, we assumed constant concentrations of ^{228}Ra over
328 depth within the water column, as shown from the depth profiles of ^{228}Ra conducted
329 at station #19 (Table 2). The same assumption was taken for ^{224}Ra in summer
330 samplings (July 2010 and June 2011), as concentrations also showed minimal
331 variation with depth. Contrarily, since ^{224}Ra concentrations decreased with depth in
332 October 2010 and March 2011 (Table 2), we used deep samples collected at station
333 #19 to characterize waters below 10 m depth. The total Ra inventories ranged from
334 $(2.0 \pm 0.1) \cdot 10^{9}$ to $(2.8 \pm 0.2) \cdot 10^{9}$ dpm for ^{224}Ra and from $(2.5 \pm 0.2) \cdot 10^{9}$ to $(3.1 \pm$
335 $0.2) \cdot 10^{9}$ dpm for ^{228}Ra, depending on the season.
336
337 Given the long half-life of ^{228}Ra, its radioactive decay in the harbor (on the order of
338 10^{6} dpm$\cdot d^{-1}$, <0.5% of the total outputs) can be neglected, but radioactive decay is a

relevant output term for the ^{224}Ra mass balance ((370 – 530)·10^{6} dpm·d^{-1}, 30 - 60% of the total outputs) (Table 4).

Ra export offshore and water age

The Ra export offshore can be determined from the excess Ra inventories in harbor waters and the apparent water age (T_w). The excess ^{224,228}Ra inventories in the harbor are calculated by subtracting the contribution of Ra from the open sea (assumed to be negligible for ^{224}Ra; for ^{228}Ra, its minimum concentration at station #32 multiplied by the harbor water volume) from the total Ra inventory in the harbor.

The apparent age of harbor waters, defined as the time a water parcel has spent since it acquired the Ra signal, can be calculated by using the variation of the activity ratios (AR) of Ra isotopes of different half-lives (Moore et al., 2006). In an environment where Ra inputs occur throughout the system and there are no losses aside from mixing with offshore seawater and radioactive decay, the residence time can be calculated as follows (Moore et al., 2006):

$$T_w = \frac{AR_{in} - AR_H}{AR_H \lambda_{224}} \quad (2)$$

where AR_{in} is the ^{224}Ra/^{228}Ra$_{ex}$ AR of the flux into the system, AR_H is the averaged ^{224}Ra/^{228}Ra$_{ex}$ AR in the harbor and λ_{224} is the decay constant of ^{224}Ra. The subscript "ex" designates the excess concentration of ^{228}Ra obtained by subtracting the concentration in open sea to the concentration in the harbor waters. The AR$_{in}$ term depends on Ra inputs from all the sources and its relative importance. The ^{224}Ra/^{228}Ra ARs for all the potential Ra sources to the harbor span a wide range: 0.9 ±

364 0.12 in water inputs from the stream, 9.5 ± 1.4 in diffusion from sediments, 5.9 ± 5.2
365 in releases from resuspension events and 1.02 ± 0.10 in SGD (see sections below).
366 Since the relative contribution of the different sources is not properly known, here we
367 used the highest $^{224}Ra/^{228}Ra_{ex}$ AR in harbor waters (3.3 ± 0.4), which was measured
368 in the inner harbor (station #3). This value shall be similar to the $^{224}Ra/^{228}Ra_{ex}$ AR in
369 the Ra source, because samples collected in the inner area of the harbor are likely
370 close to the Ra source and, thus, a minimum decay is expected. Using the weighted
371 average $^{224}Ra/^{228}Ra_{ex}$ AR of all the harbor samples (1.44 ± 0.14, 1.81 ± 0.11, 2.3 ± 0.2
372 and 2.1 ± 0.2 for July 2010, October 2010, March 2011 and June 2011, respectively),
373 the estimated seasonal apparent water ages of surface waters are 6.7 ± 1.8 d for July
374 2010, 4.2 ± 1.3 d for October 2010, 2.3 ± 1.2 d for March 2011 and 3.1 ± 1.3 d for June
375 2011.
376
377 The flux of Ra exported offshore, obtained by dividing the excess Ra inventories by
378 the water apparent age, ranged from (290 ± 80)·10^6 to (1000 ± 500)·10^6 dpm·d^{-1} for
379 ^{224}Ra and from (200 ± 60)·10^6 to (440 ± 230)·10^6 dpm·d^{-1} for ^{228}Ra, depending on the
380 season (Table 4).
381
382 *Diffusion of Ra from sediments*
383 The total diffusive fluxes of Ra from seafloor sediments to the water column of the
384 Port of Maó can be estimated from the Ra diffusive fluxes obtained from incubation
385 experiments and the area of seafloor sediments in the harbor (3.0·10^6 m^2): (340 ±
386 50)·10^6 dpm·d^{-1} for ^{224}Ra and (35 ± 2)·10^6 dpm·d^{-1} for ^{228}Ra. Since the Ra diffusive
387 fluxes estimated here are based in a single experimental value that do not take into
388 account the potential temporal and seasonal variations on these inputs, using the

uncertainty associated to this unique value seems unjustified (Garcia-Orellana et al., 2014). Thus, we assign an uncertainty of ± 50% to the resultant fluxes that shall integrate the actual variability of diffusive fluxes from sediments, as observed in other studies (Garcia-Orellana et al., 2014; Moore et al., 2008).

Ra inputs from resuspended sediments

The enhancements of short-lived Ra concentrations in the water column after sediment resuspension events (Fig. 6) are likely a consequence of Ra desorption from resuspended particles, but could also result from resuspension-induced porewater exchange with overlying waters. Considering that the docking maneuver of deep-draft vessels provokes the resuspension events (Fig. 4-5), the flux of Ra from resuspended sediments is determined from the increase of Ra inventories in the harbor after the docking of vessels and the frequency of resuspension events. Increased Ra inventories are calculated from the water volume affected by resuspension events ($2 \cdot 10^6$ m^3; determined from aerial images and bathymetry) multiplied by the enhancements of Ra concentrations in the inner harbor after vessel-driven resuspension events. To estimate this latter term, we use an average of the increase on Ra concentrations after the two vessel-driven events recorded during the 3-day intensive monitoring (5 ± 3 dpm·100L^{-1} for ^{224}Ra and 0. 9 ± 0.6 dpm·100L^{-1} for ^{228}Ra; Fig. 6). The frequency of deep draft vessels (draft > 5 m) that were docked in the harbor during the periods studied averaged 2.6, 2.0, 1.1, 1.9 vessels·d^{-1} in July 2010, October 2010, March 2011 and June 2011, respectively (data compiled from the website of Port Authority of Maó; www.portsdebalears.com). Using these data, inputs of Ra from resuspended sediments range from $120 \cdot 10^6$ to $270 \cdot 10^6$ dpm·d^{-1} for ^{224}Ra and from $15 \cdot 10^6$ to $46 \cdot 10^6$ dpm·d^{-1} for ^{228}Ra, depending on the season (Table 4).

It is difficult to accurately assess the uncertainty associated with the parameters involved in the determination of the Ra flux from resuspended sediments. Particularly, Ra enhancements derived from resuspension events can be largely variable, mainly depending on both the amount of sediments resuspended, which in turn is influenced by the vessel draft and the maneuvering procedure, and the time elapsed between resuspension events, which would determine the amount of Ra produced and available for desorption. To account for this variability and potential mischaracterization, we assign an uncertainty of ±100% to the final estimate of the Ra flux from resuspended sediments.

Inputs of Ra from stream waters

Both the concentrations of Ra dissolved and desorbed from suspended particles in stream waters need to be taken into account to estimate the inputs of Ra to the harbor waters from the stream (Moore and Shaw, 2008). The salinity (11.2, Table 3) of the sample collected on the estuarine section of the stream is high enough to assume that all Ra from suspended particles had been desorbed (Krest et al., 1999), and thus we can determine both the dissolved and desorbed Ra inputs. Since the water flow of the stream entering the inner harbor could not be precisely measured, we constrained it from the monthly precipitation in the area (Spanish Meteorological Agency, AEMET), the area draining to the stream ($2.8 \cdot 10^7$ m^2; IDEIB) and the percentage of impervious substrate (18%; IDEIB). Here it is implicitly assumed that all the precipitation falling on the impervious drainage area discharges to the stream (i.e. no further infiltration, no evaporation, no biological consumption), leading to a overestimation of the flow (flows obtained ranging from $1.9 \cdot 10^3$ to $29 \cdot 10^3$ $m^3 \cdot d^{-1}$).

438 Even considering this upper limit, the stream only contributes to a minor fraction
439 (<2%) of the total ^{224}Ra and ^{228}Ra inputs to the harbor (Table 4).
440
441 *Inputs of Ra from SGD*
442 For all the seasonal surveys, the previously evaluated Ra sources to the harbor are
443 not sufficient to balance the total Ra outputs (Table 4). These differences in Ra fluxes
444 could be reasonably ascribed to the remaining source, i.e. SGD. The estimated
445 magnitudes of the Ra fluxes derived from SGD, as well as their associated
446 uncertainties, rely on the accuracy with which the most significant components of the
447 Ra mass balance are characterized (Table 4; Fig. 7). For ^{224}Ra, these terms include Ra
448 gains by diffusion from seafloor sediments (accounting for 20 - 50% of the total
449 outputs, depending on the season) and resuspension events (10 - 40%), and losses by
450 radioactive decay (30 - 60 %) and offshore export (40 - 70%). For ^{228}Ra, sediment
451 diffusion and resuspension are lower but still relevant sources (8 - 20% and 3 - 20%,
452 respectively), whereas the only significant loss is the exported offshore (>99 %).
453
454 Inputs of Ra from SGD range from $(50 \pm 330)\cdot10^6$ dpm·d^{-1} for ^{224}Ra and $(120 \pm$
455 $80)\cdot10^6$ dpm·d^{-1} for ^{228}Ra in July 2010 to $(980 \pm 540)\cdot10^6$ dpm·d^{-1} for ^{224}Ra and (390 ±
456 230) dpm·d^{-1} for ^{228}Ra in March 2011. The propagation of the uncertainties of all the
457 components of the Ra mass balance leads to relative large uncertainties in the final
458 estimates, ranging from 50 to 600% for ^{224}Ra and from 40 to 60% for ^{228}Ra,
459 depending on the season (Table 4). The high uncertainties associated to ^{224}Ra fluxes
460 are mainly derived from the large uncertainties that were assigned to the Ra fluxes
461 from sediments, including both diffusion (uncertainty of 50%) and releases from
462 resuspension events provoked by deep draft vessels (uncertainty of 100%).

463 Contrarily, the uncertainties of the ^{228}Ra-derived estimates are mainly a consequence
464 of the uncertainties associated to the calculation of water ages (relative uncertainties
465 ranging from 30 to 50%).
466
467 **4.2. SGD to the Port of Maó**
468 The SGD flow to the Port of Maó can be estimated from the Ra flux supplied by SGD
469 derived from the mass balance and the Ra concentration in coastal groundwater (the
470 SGD end-member) (Table 4). Most of the groundwater samples were collected from
471 large wells that has not been used for long periods (up to several decades) (W1, W3,
472 W4, W5 and W7) or from large spring caves nourished by groundwater (W2 and W6).
473 Both the limited groundwater extractions and the large size of the reservoirs may
474 result in groundwater being isolated from its Ra source (aquifer solids) for long
475 periods, likely leading to decreased Ra concentrations due to radioactive decay,
476 particularly for the short-lived isotopes. This decay is indeed reflected by the low
477 ^{224}Ra/^{228}Ra AR of all these samples (< 0.7; Table 3), since groundwater commonly has
478 specific activities of ^{224}Ra and ^{228}Ra in equilibrium or even enriched in ^{224}Ra relative
479 to ^{228}Ra, due to alpha recoil and/or the faster regeneration of ^{224}Ra (Charette et al.,
480 2003; Porcelli and Swarzenski, 2003; Rama and Moore, 1996; Swarzenski, 2007).
481 Therefore, these groundwater samples would not be appropriate for the
482 characterization of Ra concentrations in SGD discharging to the Port of Maó. From all
483 the sites sampled, W8 is the only one where groundwater is continuously flowing,
484 since it is a near-shore well (10 m from the harbor waters) frequently (almost daily)
485 pumped for commercial purposes. Additionally, we purged the well (extracting
486 hundreds of liters) before sampling to ensure that groundwater was completely
487 renewed. Groundwater samples collected from this well are thus the best

488 representation we have of the Ra concentration in the SGD end-member. Average Ra
489 concentration collected from W8 are 224 ± 13 dpm·100L^{-1} for ^{224}Ra and 220 ± 20
490 dpm·100L^{-1} for ^{228}Ra, with an ^{224}Ra/^{228}Ra AR of ~1 (Table 3). ^{226}Ra concentrations in
491 this well are considerably lower (2 times) than ^{228}Ra concentrations, justifying the
492 low ^{226}Ra enrichment observed in harbor waters.
493
494 Results of the SGD fluxes derived from the ^{224,228}Ra mass balance and Ra
495 concentrations measured in groundwater from W8 are shown in Table 4. For most of
496 the seasonal samplings, SGD flows derived from ^{224}Ra are nominally higher (by a
497 factor of ~2) than those obtained when using ^{228}Ra, although the values overlap
498 within the uncertainties. The most likely reason for the differences in the SGD flows is
499 the difficulty in the characterization of the sedimentary source, including the Ra
500 supplied from both diffusion and resuspension events. The characterization of the Ra
501 inputs from sediments have a larger influence for ^{224}Ra than for ^{228}Ra, given its
502 relative importance in the mass balance (Fig. 7). Indeed, this is reflected in the larger
503 uncertainties associated with ^{224}Ra-derived SGD rates. SGD flows obtained from ^{228}Ra
504 would thus be more reliable, as they are less conditioned on the appropriate
505 characterization of the Ra fluxes from diffusion and resuspension events. Although
506 calculations are not reported in the manuscript, ^{223}Ra-derived SGD is also comparable
507 to the flows obtained when using ^{224}Ra and ^{228}Ra, but its large uncertainty (70 -
508 800%) prevents any detailed evaluation.
509
510 Based only on the ^{228}Ra-derived estimates, SGD presents a seasonal pattern likely
511 dominated by changes in precipitation over the annual cycle, with maximum SGD
512 rates in wet seasons ((180 ± 100)·10^3 m^3·d^{-1} in March11) and minimum flows in the

513 dry period ((56 ± 35)·10^3 $m^3 \cdot d^{-1}$ in July10). The seasonal discharge pattern is in phase
514 with the recharge cycle of the aquifers with maximum annual precipitations in spring
515 and fall, suggesting a rapid response of the limestone aquifer to precipitation events,
516 as previously reported in other Mediterranean coastal areas (Garcia-Solsona et al.,
517 2010b; Rodellas et al., 2012). Variations in precipitation may also lead to seasonal
518 oscillation in the freshwater-seawater interface, driving the discharge of both fresh
519 groundwater and seawater previously infiltrated to the coastal aquifer (Michael et al.,
520 2005). However, the low salinities measured in most of the wells located close to the
521 harbor suggest that SGD into the Port of Maó likely contains a minor fraction of saline
522 groundwater. Given the micro-tidal conditions of the Port of Maó (10-30 cm), no
523 major tidal modulation in the harbor is expected. When normalizing the estimated
524 SGD to the harbor shore length (~18 km), the annual SGD flow is ((1.1 – 3.6)·10^6
525 $m^3 \cdot yr^{-1} \cdot km^{-1}$), which is in good agreement with other estimates for Mediterranean
526 islands (Garcia-Solsona et al., 2010a; Moore, 2006; Rodellas et al., 2014; Tovar-
527 Sanchez et al., 2014).
528
529 **4.3. Sediment influence on Ra mass balances**
530 The Ra mass balance conducted in the Port of Maó reveals that the Ra flux from
531 sediments, including both diffusion and releases from resuspension events,
532 represents a significant source of Ra to the harbor waters (Table 4; Fig. 7). This
533 sedimentary source accounts for a major fraction of the ^{224}Ra supplied to the system,
534 particularly in summer, when SGD fluxes are minimal and the resuspension events
535 are more frequent. For instance, while the sediment source represents 30% of the
536 total inputs of ^{224}Ra in March 2011, it is the dominant (90%) source in July 2010 (Fig.
537 7). The influence of sediments on the ^{228}Ra mass balance is lower but still significant,

538 ranging from 10% of the total ^{228}Ra inputs in March 2011 to 40% in July 2010 (Fig. 7).
539 These differences in the relative importance of sediments for ^{224}Ra and ^{228}Ra are
540 mainly related to differences in their production rates, which are set by their decay
541 constants (Charette et al., 2008). Short-time and small scale processes, such as
542 diffusion from seafloor sediments or daily sediment resuspension events, do not
543 allow a significant ingrowth of long-lived Ra isotopes, resulting in relatively low
544 fluxes to the water column compared to short-lived Ra isotopes (King, 2012; Santos et
545 al., 2012).
546
547 Unlike the results that we obtained in the Port of Maó, fluxes from seafloor sediments
548 are commonly a minor source of Ra isotopes compared to the Ra inputs derived from
549 SGD (e.g. Rama and Moore 1996; Charette et al. 2003; Beck et al. 2007; Garcia-Solsona
550 et al. 2008b; Rodellas et al. 2012), particularly when coarse-grained sediments are
551 involved, since they represent a relatively low surface area substrate with low Ra
552 pools available for adsorption-desorption reactions (Beck and Cochran 2013).
553 However, sediments can represent a relevant source of Ra isotopes in those systems
554 covered by fine-grained sediments and/or affected by processes that favor Ra
555 exchange across the sediment-water interface, such as bioirrigation, sediment
556 resuspension, seasonal hypoxia or short-scale (mm to cm) porewater exchange
557 driven by pressure gradients (Breier et al., 2010, 2009; Colbert and Hammond, 2008;
558 Garcia-Orellana et al., 2014; Gleeson et al., 2013), as we also showed in this work. In
559 addition, Ra inputs from sediments can also be relevant and comparable to those
560 gains from SGD in large scale studies, such as those conducted in entire basins where
561 inputs from the entire continental shelf must be considered (Moore et al.
562 2008;Rodellas et al., submitted). In all these environments, the estimation of SGD

563 relies on an appropriate characterization of Ra fluxes from sediment sources.
564 However, Ra flux from sediments might be difficult to quantify, since it depends on
565 several parameters highly variable in space (e.g. sediment grain size, porosity, redox
566 state) and time (e.g. amount of sediments resuspended, frequency of resuspension
567 events, bioturbation) (Breier et al., 2010; Garcia-Orellana et al., 2014; Moore et al.,
568 2008). For instance, Moore et al. (2008) showed that Ra fluxes from fine-grained
569 sediments are commonly 1-2 orders of magnitude higher than those from coarse-
570 grained sediments, requiring a detailed knowledge of the relative extension of each
571 type of sediment . Also, Garcia-Orellana et al. (2014) suggested that seasonally
572 variable bioirrigation and Mn cycling may exert important controls on the Ra flux
573 from seafloor sediments, resulting in seasonally variable Ra diffusive fluxes. Thus,
574 estimates of Ra inputs from sediments based on several assumptions and limited
575 measurements might not adequately represent spatial or temporal variations of the
576 sediment sources. As done in this study, when Ra inputs from sediment can not be
577 accurately characterized, large uncertainties need to be assigned to the inputs from
578 sediments, which shall integrate the actual contribution of Ra isotopes from
579 sediments, although introduce large uncertainties to the final SGD estimates. Since
580 sediment sources are greater in proportion and magnitude for short-lived Ra isotopes
581 than for the long-lived ones, failure to estimate the long-lived Ra fluxes from
582 sediments is smoothed out by their minor influence on the final SGD estimate.
583 Accordingly, in those systems where sediments can represent a major contributor to
584 the Ra mass balance (e.g. shallow water bodies, fine-grained systems or areas prone
585 to bioturbation or resuspension events), long-lived isotopes are likely the most
586 appropriate Ra tracers of SGD. Yet, given that Ra isotopes reflect input mechanisms
587 on time scales similar to their regeneration rates, the selection of the appropriate Ra

588 tracer would also depend on the target processes of the study (King, 2012; Santos et
589 al., 2012). For instance, using long-lived Ra isotopes may not capture short (days)
590 scale recirculation processes, such as tidally-driven SGD.

CONCLUSIONS

Submarine Groundwater Discharge (SGD) to the Port of Maó has been estimated by using a comprehensive mass balance of ^{224}Ra and ^{228}Ra. The results show that the Ra flux from sediments, through diffusion and releases associated to resuspension events, represents a significant source of Ra to the harbor waters. Difficulties in accurately estimating the Ra fluxes from sediments, which account for 30 - 90% and 10 - 40% of the ^{224}Ra and ^{228}Ra supplied to the system, respectively, result on large uncertainties on the final SGD estimates. Uncertainties are particularly high for ^{224}Ra, given the larger relative importance of the sediment-derived inputs in the Ra mass balance because of its faster production rate in sediments. Based on ^{228}Ra, the SGD flows to the Port of Maó range from $(56 \pm 35)\cdot10^3$ to $(180 \pm 100)\cdot10^3$ $m^3\cdot d^{-1}$, showing a seasonality likely dominated by the recharge cycle. Findings derived from this work are evidence that attributing Ra inputs to the water column solely to SGD in systems where sediments may play a relevant role (e.g. shallow water bodies, muddy systems or areas prone to bioturbation or resuspension events) might not be accurate, requiring a detailed evaluation of the sediment source. Since inputs from sediments are often difficult to quantify, using long-lived Ra isotopes to estimate the SGD flow may minimize the effect of a poor characterization of the sediment source.

Besides the influence of sediments as a source of Ra isotopes to the water column of the Port of Maó, harbor sediments could also represent a relevant source of other compounds, such as major nutrients (e.g. nitrogen or phosphorous) or heavy metals (e.g. Cu, Pb, Hg), to the harbor waters. Inputs of metals from seafloor sediments may be particularly relevant in the Port of Maó, because sediments contain significant amounts of metals as a consequence of industrial and urban activities (Garcia-

Orellana et al., 2011). Considering its frequency and magnitude, the resuspension of seafloor sediments triggered by vessel docking maneuvers could represent a major mechanism favoring the release of sediment-bound metals into the water column (Kalnejais et al., 2010; Superville et al., 2014). Inputs of metals from sediments may have profound implications on the biogeochemical cycles of the water column, by limiting algal growth or acting as toxic agents (Lafabrie et al., 2013; Morel and Price, 2003; Twining and Baines, 2013). Thus, fluxes of trace metals from sediments, as well as the effects of the sediment sources on the phytoplankton composition or growth, should be further studied.

Acknowledgments

This project has been partially funded by the Spanish Government project EHRE (ref. CTM2009-08270). V.R. acknowledges financial support through a PhD fellowship (AP2008-03044) from MICINN (Spain). Authors want to thank the support of the Generalitat de Catalunya to MERS (2014 SGR-1356). Support for the research of P.M. was received through the prize ICREA Academia, funded by the Generalitat de Catalunya and by a Gledden Visiting Fellowship awarded by the Institute of Advanced Studies at the University of Western Australia. We would like to gratefully acknowledge the Port Authority of Maó and OBSAM for their collaboration. We thank G. Basterretxea, A. Tovar-Sánchez, A. Jordi and our colleagues at the Laboratori de Radioactivitat Ambiental (UAB) and the IMEDEA for their comments, help and assistance during field and lab work.

638 **REFERENCES**

639 Agrawal, Y.C., Pottsmith, H.C., 2000. Instruments for particle size and settling velocity
640 observations in sediment transport. Mar. Geol. 168, 89–114. doi:10.1016/S0025-
641 3227(00)00044-X

642 Beck, A.J., Cochran, M.A., 2013. Controls on solid-solution partitioning of radium in
643 saturated marine sands. Mar. Chem. 156, 38–48.
644 doi:10.1016/j.marchem.2013.01.008

645 Beck, A.J., Rapaglia, J.P., Cochran, J.K., Bokuniewicz, H.J., 2007. Radium mass-balance
646 in Jamaica Bay, NY: Evidence for a substantial flux of submarine groundwater.
647 Mar. Chem. 106, 419–441. doi:10.1016/j.marchem.2007.03.008

648 Breier, J.A., Breier, C.F., Edmonds, H.N., 2010. Seasonal dynamics of dissolved Ra
649 isotopes in the semi-arid bays of south Texas. Mar. Chem. 122, 39–50.
650 doi:10.1016/j.marchem.2010.08.008

651 Breier, J.A., Nidzieko, N., Monismith, S., Moore, W., Paytan, A., 2009. Tidally regulated
652 chemical fluxes across the sediment-water interface in elkhorn slough, california:
653 Evidence from a coupled geochemical and hydrodynamic approach. Limnol.
654 Oceanogr. 54, 1964–1980.

655 Burnett, W.C., Bokuniewicz, H., Huettel, M., Moore, W.S., Taniguchi, M., 2003.
656 Groundwater and pore water inputs to the coastal zone. Biogeochemistry 66, 3–
657 33. doi:10.1023/B:BIOG.0000006066.21240.53

658 Cai, W.-J., Wang, Y., Krest, J., Moore, W.S., 2003. The geochemistry of dissolved
659 inorganic carbon in a surficial groundwater aquifer in North Inlet, South
660 Carolina, and the carbon fluxes to the coastal ocean. Geochim. Cosmochim. Acta
661 67, 631–639. doi:10.1016/S0016-7037(02)01167-5

662 Charette, M.A., Buesseler, K.O., Andrews, J.E., 2001. Utility of radium isotopes for
663 evaluating the input and transport of groundwater-derived nitrogen to a Cape
664 Cod estuary. Limnol. Oceanogr. 46, 465–470.

665 Charette, M.A., Henderson, P.B., Breier, C.F., Liu, Q., 2013. Submarine groundwater
666 discharge in a river-dominated Florida estuary. Mar. Chem. 156, 3–17.
667 doi:10.1016/j.marchem.2013.04.001

668 Charette, M.A., Moore, W.S., Burnett, W.C., 2008. Uranium- and Thorium-Series
669 Nuclides as Tracers of Submarine Groundwater Discharge (in U-Th Series
670 Nuclides in Aquatic Systems), in: Radioactivity in the Environment, Radioactivity
671 in the Environment. Elsevier, pp. 155–191. doi:10.1016/S1569-4860(07)00005-
672 8

673 Charette, M.A., Splivallo, R., Herbold, C., Bollinger, M.S., Moore, W.S., 2003. Salt marsh
674 submarine groundwater discharge as traced by radium isotopes. Mar. Chem. 84,
675 113–121. doi:10.1016/j.marchem.2003.07.001

676 Colbert, S.L., Hammond, D.E., 2008. Shoreline and seafloor fluxes of water and short-
677 lived Ra isotopes to surface water of San Pedro Bay, CA. Mar. Chem. 108, 1–17.
678 doi:10.1016/j.marchem.2007.09.004

679 Dulaiova, H., Burnett, W.C., Chanton, J.P., Moore, W.S., Bokuniewicz, H.J., Charette,
680 M.A., Sholkovitz, E., 2006. Assessment of groundwater discharges into West Neck
681 Bay, New York, via natural tracers. Cont. Shelf Res. 26, 1971–1983.
682 doi:10.1016/j.csr.2006.07.011

683 Fayas, J., 1972. Estudio de los recursos hidráulicos totales de la isla de Menorca. Serv.
684 Geológico Obras Públicas I, Madrid.

685 Fornós, J.J., Obradors, A., Rosell, V.M., 2004. Història Natural del Migjorn de Mallorca.
686 Soc. d'Història Nat. les Balear. 11, 1–378.

687 Garcia-Orellana, J., Cañas, L., Masqué, P., Obrador, B., Olid, C., Pretus, J., 2011.
688 Chronological reconstruction of metal contamination in the Port of Maó
689 (Minorca, Spain). Mar. Pollut. Bull. 62, 1632–40.
690 doi:10.1016/j.marpolbul.2011.06.013

691 Garcia-Orellana, J., Cochran, J.K., Bokuniewicz, H., Daniel, J.W.R., Rodellas, V., Heilbrun,
692 C., 2014. Evaluation of 224Ra as a tracer for submarine groundwater discharge
693 in Long Island Sound (NY). Geochim. Cosmochim. Acta 141, 314–330.
694 doi:10.1016/j.gca.2014.05.009

695 Garcia-Orellana, J., Rodellas, V., Casacuberta, N., Lopez-Castillo, E., Vilarrasa, M.,
696 Moreno, V., Garcia-Solsona, E., Masqué, P., 2013. Submarine groundwater
697 discharge: Natural radioactivity accumulation in a wetland ecosystem. Mar.
698 Chem. 156, 61–72. doi:10.1016/j.marchem.2013.02.004

699 Garcia-Solsona, E., Garcia-Orellana, J., Masqué, P., Dulaiova, H., 2008a. Uncertainties
700 associated with 223Ra and 224Ra measurements in water via a Delayed
701 Coincidence Counter (RaDeCC). Mar. Chem. 109, 198–219.
702 doi:10.1016/j.marchem.2007.11.006

703 Garcia-Solsona, E., Garcia-Orellana, J., Masqué, P., Garcés, E., Radakovitch, O., Mayer,
704 A., Estradé, S., Basterretxea, G., 2010a. An assessment of karstic submarine
705 groundwater and associated nutrient discharge to a Mediterranean coastal area
706 (Balearic Islands, Spain) using radium isotopes. Biogeochemistry 97, 211–229.
707 doi:10.1007/s10533-009-9368-y

708 Garcia-Solsona, E., Garcia-Orellana, J., Masqué, P., Rodellas, V., Mejías, M., Ballesteros,
709 B., Domínguez, J.A., 2010b. Groundwater and nutrient discharge through karstic
710 coastal springs (*Castelló*, Spain). Biogeosciences 7, 2625–2638. doi:10.5194/bg-
711 7-2625-2010

712 Garcia-Solsona, E., Masqué, P., Garcia-Orellana, J., Rapaglia, J., Beck, A.J., Cochran, J.K.,
713 Bokuniewicz, H.J., Zaggia, L., Collavini, F., 2008b. Estimating submarine
714 groundwater discharge around Isola La Cura, northern Venice Lagoon (Italy), by

715 using the radium quartet. Mar. Chem. 109, 292–306.
716 doi:10.1016/j.marchem.2008.02.007

717 Gleeson, J., Santos, I.R., Maher, D.T., Golsby-Smith, L., 2013. Groundwater–surface
718 water exchange in a mangrove tidal creek: Evidence from natural geochemical
719 tracers and implications for nutrient budgets. Mar. Chem. 156, 27–37.
720 doi:10.1016/j.marchem.2013.02.001

721 IDEIB, n.d. IDEIB Infraestructura de dades espacials de les Illes Balears. Govern de les
722 llles Balears. [WWW Document]. URL www.ideib.caib.es/visualitzador (accessed
723 3.20.14).

724 Kalnejais, L.H., Martin, W.R., Bothner, M.H., 2010. The release of dissolved nutrients
725 and metals from coastal sediments due to resuspension. Mar. Chem. 121, 224–
726 235. doi:10.1016/j.marchem.2010.05.002

727 King, J.N., 2012. Synthesis of benthic flux components in the Patos Lagoon coastal
728 zone, Rio Grande do Sul, Brazil. Water Resour. Res. 48.
729 doi:10.1029/2011WR011477

730 Krest, J.M., Moore, W.S., Rama, 1999. and in the mixing zones of the Mississippi and
731 Atchafalaya Rivers: indicators of groundwater input. Mar. Chem. 64, 129–152.
732 doi:10.1016/S0304-4203(98)00070-X

733 Lafabrie, C., Garrido, M., Leboulanger, C., Cecchi, P., Grégori, G., Pasqualini, V.,
734 Pringault, O., 2013. Impact of contaminated-sediment resuspension on
735 phytoplankton in the Biguglia lagoon (Corsica, Mediterranean Sea). Estuar. Coast.
736 Shelf Sci. 130, 70–80. doi:10.1016/j.ecss.2013.06.025

737 Michael, H.A., Mulligan, A.E., Harvey, C.F., 2005. Seasonal oscillations in water
738 exchange between aquifers and the coastal ocean. Nature 436, 1145–8.
739 doi:10.1038/nature03935

740 Moore, W.S., 2003. Sources and fluxes of submarine groundwater discharge
741 delineated by radium isotopes. Biogeochemistry 66, 75–93.
742 doi:10.1023/B:BIOG.0000006065.77764.a0

743 Moore, W.S., 2006. Radium isotopes as tracers of submarine groundwater discharge
744 in Sicily. Cont. Shelf Res. 26, 852–861. doi:10.1016/j.csr.2005.12.004

745 Moore, W.S., 2010. The Effect of Submarine Groundwater Discharge on the Ocean.
746 Ann. Rev. Mar. Sci. 2, 59–88. doi:10.1146/annurev-marine-120308-081019

747 Moore, W.S., Arnold, R., 1996. Measurement of223Ra and224Ra in coastal waters
748 using a delayed coincidence counter. J. Geophys. Res. C Ocean. 101, 1321–1329.
749 doi:10.1029/95JC03139

750 Moore, W.S., Blanton, J.O., Joye, S.B., 2006. Estimates of flushing times, submarine
751 groundwater discharge, and nutrient fluxes to Okatee Estuary, South Carolina. J.
752 Geophys. Res. 111, C09006. doi:10.1029/2005JC003041

753 Moore, W.S., Reid, D.F., 1973. Extraction of radium from natural waters using
754 manganese-impregnated acrylic fibers. J. Geophys. Res. 78, 8880–8886.
755 doi:10.1029/JC078i036p08880

756 Moore, W.S., Sarmiento, J.L., Key, R.M., 2008. Submarine groundwater discharge
757 revealed by 228Ra distribution in the upper Atlantic Ocean. Nat. Geosci. 1, 309–
758 311. doi:10.1038/ngeo183

759 Moore, W.S., Shaw, T.J., 2008. Fluxes and behavior of radium isotopes, barium, and
760 uranium in seven Southeastern US rivers and estuaries. Mar. Chem. 108, 236–
761 254. doi:10.1016/j.marchem.2007.03.004

762 Morel, F.M.M., Price, N.M., 2003. The biogeochemical cycles of trace metals in the
763 oceans. Science 300, 944–7. doi:10.1126/science.1083545

764 Porcelli, D., Swarzenski, P., 2003. The behavior of U-and Th-series nuclides in
765 groundwater. Rev. Mineral. Geochemistry 52, 317–361.

766 Rama, P.S., Moore, W.S., 1996. Using the radium quartet for evaluating groundwater
767 input and water exchange in salt marshes. Geochim. Cosmochim. Acta 60, 4645–
768 4652. doi:10.1016/S0016-7037(96)00289-X

769 Rodellas, V., Garcia-Orellana, J., Garcia-Solsona, E., Masqué, P., Domínguez, J.A.,
770 Ballesteros, B.J., Mejías, M., Zarroca, M., 2012. Quantifying groundwater discharge
771 from different sources into a Mediterranean wetland by using 222Rn and Ra
772 isotopes. J. Hydrol. 466-467, 11–22. doi:10.1016/j.jhydrol.2012.07.005

773 Rodellas, V., Garcia-Orellana, J., Tovar-Sánchez, A., Basterretxea, G., López-Garcia, J.M.,
774 Sánchez-Quiles, D., Garcia-Solsona, E., Masqué, P., 2014. Submarine groundwater
775 discharge as a source of nutrients and trace metals in a Mediterranean Bay
776 (Palma Beach, Balearic Islands). Mar. Chem. 160, 56–66.
777 doi:10.1016/j.marchem.2014.01.007

778 Santos, I.R., Eyre, B.D., Huettel, M., 2012. The driving forces of porewater and
779 groundwater flow in permeable coastal sediments: A review. Estuar. Coast. Shelf
780 Sci. 98, 1–15. doi:10.1016/j.ecss.2011.10.024

781 Slomp, C.P., Van Cappellen, P., 2004. Nutrient inputs to the coastal ocean through
782 submarine groundwater discharge: controls and potential impact. J. Hydrol. 295,
783 64–86. doi:10.1016/j.jhydrol.2004.02.018

784 Sun, Y., Torgersen, T., 1998. The effects of water content and Mn-fiber surface
785 conditions on measurement by emanation. Mar. Chem. 62, 299–306.
786 doi:10.1016/S0304-4203(98)00019-X

787 Superville, P.-J., Prygiel, E., Magnier, A., Lesven, L., Gao, Y., Baeyens, W., Ouddane, B.,
788 Dumoulin, D., Billon, G., 2014. Daily variations of Zn and Pb concentrations in the
789 Deûle River in relation to the resuspension of heavily polluted sediments. Sci.
790 Total Environ. 470-471, 600–7. doi:10.1016/j.scitotenv.2013.10.015

791 Swarzenski, P.W., 2007. U/Th series radionuclides as coastal groundwater tracers.
792 Chem. Rev. 107, 663–74. doi:10.1021/cr0503761

793 Tovar-Sanchez, A., Basterretxea, G., Rodellas, V., Sánchez-Quiles, D., Garcia-Orellana, J.,
794 Masqué, P., Jordi, A., López, J.M., Garcia Solsona, E., 2014. Contribution of
795 groundwater discharge to the coastal dissolved nutrients and trace metal
796 concentrations in Majorca Island: karstic vs detrital systems. Environ. Sci.
797 Technol. 48, 11819–11827. doi:10.1021/es502958t

798 Twining, B.S., Baines, S.B., 2013. The trace metal composition of marine
799 phytoplankton. Ann. Rev. Mar. Sci. 5, 191–215. doi:10.1146/annurev-marine-
800 121211-172322

801 Windom, H.L., Moore, W.S., Niencheski, L.F.H., Jahnke, R.A., 2006. Submarine
802 groundwater discharge: A large, previously unrecognized source of dissolved
803 iron to the South Atlantic Ocean. Mar. Chem. 102, 252–266.
804 doi:10.1016/j.marchem.2006.06.016

805

806

807 **TABLES**

808 **Table 1.** Average Ra concentrations in surface waters of the inner harbor (stations #1
809 to #4) and at the offshore station (#32). Ratios between Ra concentrations in and out
810 of the harbor are also shown.

		^{223}Ra	^{224}Ra	^{226}Ra	^{228}Ra
		dpm·100L^{-1}			
July 2010	Inner Harbor	1.31 ± 0.15	11.7 ± 1.3	13.7 ± 0.7	9.6 ± 1.1
	Offshore	0.08 ± 0.03	0.2 ± 0.2	13.7 ± 0.5	3.8 ± 0.7
	In/Out ratio	16	51	1.0	2.5
October 2010	Inner Harbor	1.24 ± 0.08	14 ± 2	12.2 ± 1.4	9.9 ± 1.0
	Offshore	0.18 ± 0.08	2.0 ± 0.3	9.1 ± 0.4	4.1 ± 0.6
	In/Out ratio	6.9	6.9	1.3	2.4
March 2011	Inner Harbor	0.77 ± 0.18	7.9 ± 1.4	11 ± 2	6.7 ± 0.3
	Seawater	0.20 ± 0.06	2.0 ± 0.3	12.8 ± 0.4	3.7 ± 0.5
	In/Out ratio	3.8	3.9	0.8	1.8
June 2011	Inner Harbor	0.96 ± 0.21	9.1 ± 1.3	12 ± 2	7.4 ± 0.8
	Seawater	0.10 ± 0.04	0.3 ± 0.2	12.6 ± 0.5	4.0 ± 0.8
	In/Out ratio	9.6	28	1.0	1.9

811

812

813

814 **Table 2.** ^{224}Ra and ^{228}Ra concentrations in the depth profile conducted at station #19

815 in October 2010, March 2011 and June 2011.

	Depth	Salinity	^{224}Ra	^{228}Ra
	m		dpm·100L^{-1}	
October10	1	37.89	6.3 ± 0.6	6.3 ± 0.7
	5	37.90	5.6 ± 0.6	5.3 ± 0.9
	15	37.90	2.4 ± 0.5	6.0 ± 1.2
	25	37.91	2.0 ± 0.4	6.7 ± 1.5
March11	1	37.59	5.1 ± 0.5	5.8 ± 0.8
	10	37.73	3.8 ± 0.6	6.0 ± 1.1
	20	37.80	2.8 ± 0.5	6.2 ± 0.9
June11	1	37.62	4.4 ± 0.4	6.6 ± 0.6
	10	37.61	3.4 ± 0.4	5.3 ± 1.4
	20	37.65	4.4 ± 0.5	7.6 ± 1.5

816
817
818

819

820 **Table 3.** Average Ra concentrations in groundwater samples and in the freshwater

821 (Stream-F) and estuarine regions (Stream-F) of the inflowing stream (uncertainties

822 represent the standard deviation).

823

	Sal	^{223}Ra	^{224}Ra	^{226}Ra	^{228}Ra	^{224}Ra/^{228}Ra AR
		dpm·100L^{-1}				
W1	1.6	1.5 ± 0.8	23 ± 11	11.6 ± 1.0*	21 ± 2*	0.53 ± 0.05*
W2	0.8	1.7 ± 0.2	16 ± 4	49 ± 2*	46 ± 2*	0.26 ± 0.02*
W3	1.4	7.4 ± 2.5	66 ± 11	160 ± 3*	115 ± 5*	0.59 ± 0.05*
W4	1.1	1.7 ± 1.5	31 ± 20	52 ± 2*	33 ± 2*	0.50 ± 0.04*
W5	8.9	5.1 ± 0.6	165 ± 13	71 ± 5*	230 ± 20*	0.67 ± 0.08*
W6	0.7	1.22 ± 0.05	27 ± 2	33 ± 2*	231 ± 4*	0.12 ± 0.01*
W7	12.6	1.5 ± 0.2*	26 ± 2*	100 ± 2*	58 ± 5*	0.46 ± 0.05*
W8	0.8	8.4 ± 2.1	224 ± 13	107 ± 11	220 ± 20	1.02 ± 0.10
Stream-F	0.9	0.70 ± 0.09*	11.4 ± 0.8*	n.a.	n.a.	n.a.
Stream-E	11.2	0.50 ± 0.11*	17.3 ± 1.1*	9.0 ± 0.8*	20 ± 3*	0.85 ± 0.12*

824 n.a. not analyzed

825 * Only measured in one survey: analytical uncertainties are reported

826

827

828 **Table 4.** Inputs and outputs of ^{224}Ra and ^{228}Ra to the Port of Maó for all the four
829 surveys. Difference between inputs and outputs is used to derive the flux of Ra from
830 SGD and the final SGD estimate.
831

	July 2010		October 2010		March 2011		June 2011		
	^{224}Ra	^{228}Ra	^{224}Ra	^{228}Ra	^{224}Ra	^{228}Ra	^{224}Ra	^{228}Ra	Units
Export offshore	290 ± 80	200 ± 60	660 ± 210	370 ± 110	1000 ± 500	440 ± 230	720 ± 300	350 ± 150	$\cdot 10^6$ dpm·d^{-1}
Decay	370 ± 11	0.95 ± 0.04	528 ± 13	1.01 ± 0.03	438 ± 13	0.84 ± 0.03	418 ± 11	0.86 ± 0.04	$\cdot 10^6$ dpm·d^{-1}
TOTAL OUPUTS	660 ± 80	200 ± 60	1200 ± 200	370 ± 120	1400 ± 500	440 ± 220	1100 ± 300	350 ± 150	$\cdot 10^6$ dpm·d^{-1}
Sediments diffusion	340 ± 170	35 ± 18	340 ± 170	35 ± 18	340 ± 170	35 ± 18	340 ± 170	35 ± 18	$\cdot 10^6$ dpm·d^{-1}
Sediment resuspension	270 ± 270	46 ± 46	210 ± 210	26 ± 26	120 ± 120	15 ± 15	200 ± 200	24 ± 24	$\cdot 10^6$ dpm·d^{-1}
Stream	0.33 ± 0.02	0.39 ± 0.05	5.0 ± 0.3	5.8 ± 0.7	1.35 ± 0.09	1.6 ± 0.2	0.55 ± 0.04	0.65 ± 0.08	$\cdot 10^6$ dpm·d^{-1}
TOTAL INPUTS	610 ± 320	82 ± 49	550 ± 270	67 ± 32	460 ± 210	52 ± 23	530 ± 260	60 ± 30	$\cdot 10^6$ dpm·d^{-1}
SGD	50 ± 330	120 ± 80	630 ± 340	300 ± 120	980 ± 540	390 ± 230	610 ± 400	290 ± 150	$\cdot 10^6$ dpm·d^{-1}
SGD flow	20 ± 150	56 ± 35	280 ± 150	140 ± 60	440 ± 240	180 ± 100	270 ± 180	130 ± 70	$\cdot 10^3$ m^3·d^{-1}

832
833
834

835 **FIGURE LEGENDS**

836 **Figure 1.** Map of the Port of Maó including the location of all the hydrographic
837 stations and the site where the three-day monitoring was conducted. The location of
838 the groundwater samples, the inflowing stream and the sediment core collected are
839 also shown. Dashed-lines differentiate (from the left to the right) the inner, middle
840 and outer areas of the harbor, and the boundary of the study site.

841

842 **Figure 2.** Salinity distribution on a cross section along the Port of Maó derived from
843 CTD profiles conducted in each station. The dashed line highlights the boundary of
844 the harbor.

845

846 **Figure 3**. Ra concentrations in surface waters along the harbor for all the four
847 surveys conducted. Average uncertainties associated to Ra concentrations are 0.1,
848 0.5, 0.7 and 0.8 dpm·100L^{-1} for ^{223}Ra, ^{224}Ra, ^{226}Ra and ^{228}Ra, respectively. Stations #29
849 and #32 are outside the harbor.

850

851 **Figure 4**. Resuspension of sediments produced by the undocking maneuver of a
852 vessel (draft ~6 m) departing from the Port of Maó.

853

854 **Figure 5.** Concentration of suspended particles (in µL·L^{-1}) in waters of the inner part
855 of the harbor recorded during two days by laser in situ scattering and
856 transmissometry (LISST). Black lines represent the depth profiles conducted by LISST
857 and used to derive the interpolation. The maneuvering of the deep draft vessel to
858 dock and undock is represented with a white dashed-line. Notice that no

859 measurements were conducted after the resuspension events occurred at the third
860 day of monitoring.
861
862 **Figure 6**. Variation of the Ra concentrations in surface waters of the inner part of the
863 harbor recorded during the three-day intensive monitoring. Grey areas reflect the
864 maneuvering of deep draft vessels to dock. Average uncertainties associated to Ra
865 concentrations are 0.1, 0.7, 0.8 and 0.8 dpm·100L^{-1} for ^{223}Ra, ^{224}Ra, ^{226}Ra and ^{228}Ra,
866 respectively. Ra concentrations and patterns in deep waters were similar to those
867 shown for surface waters.
868
869 **Figure 7**. Contribution of different sources (diffusion from sediments, sediment
870 resuspension events, stream discharge and SGD) to the ^{224}Ra and ^{228}Ra total inputs to
871 the Port of Maó in all the seasonal surveys conducted.
872

873 **FIGURE 1**

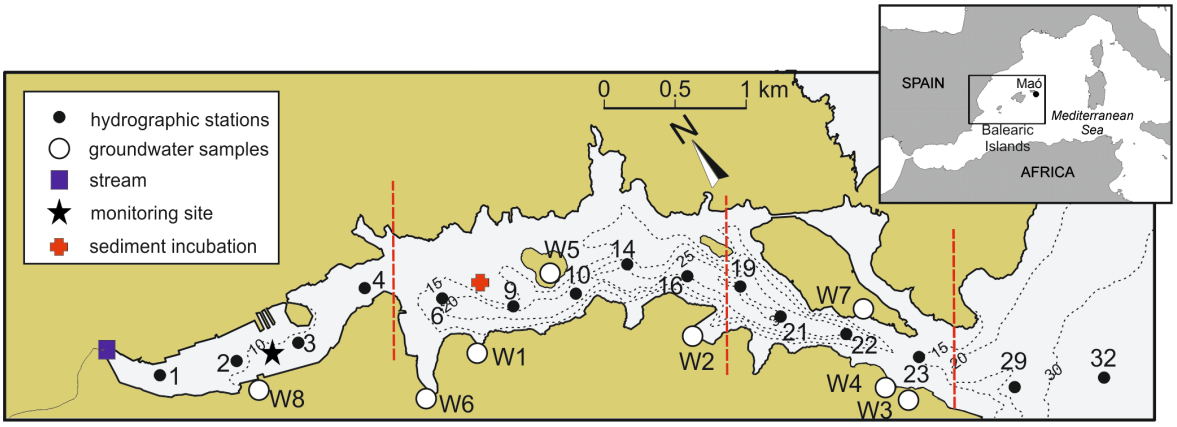

874

875 **FIGURE 2**

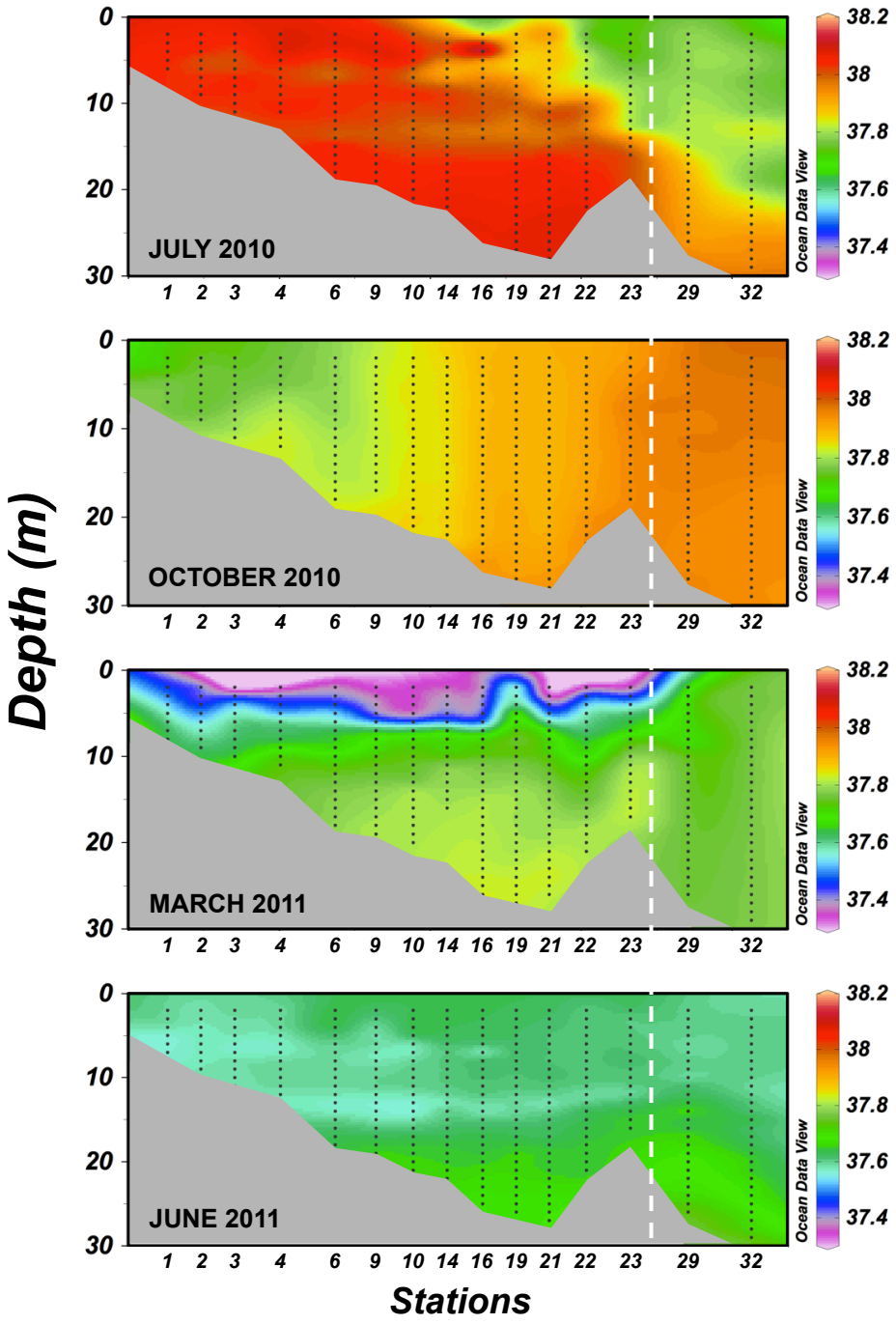

876

877 **FIGURE 3**

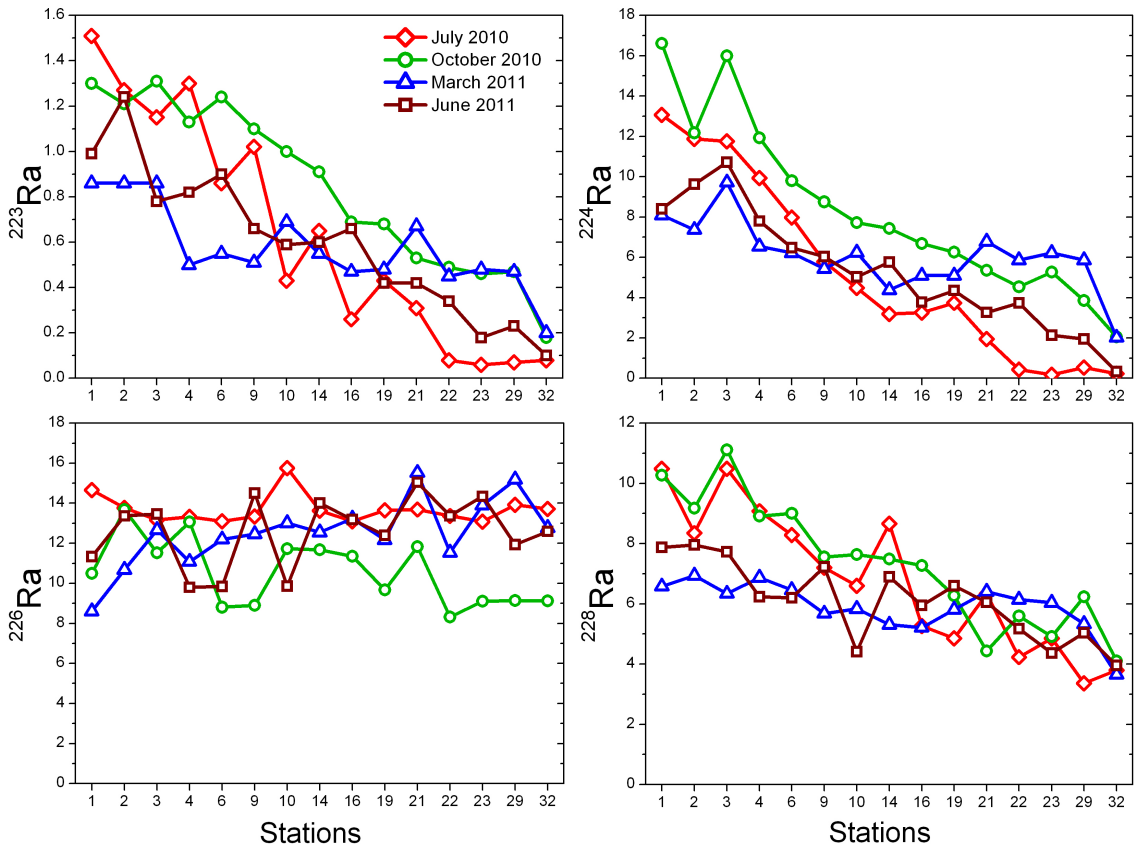

878

FIGURE 4

881 **FIGURE 5**

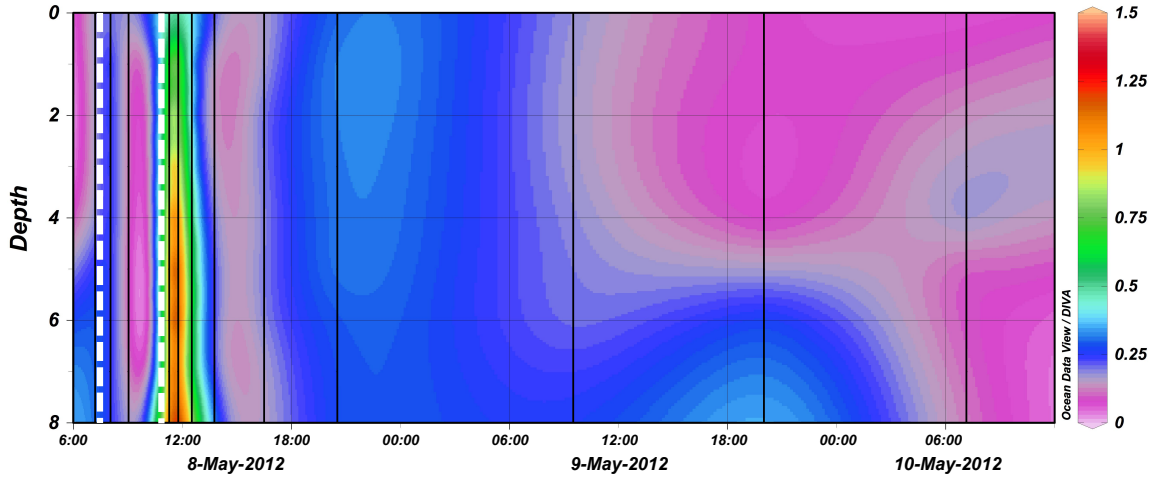

882

883 **FIGURE 6**

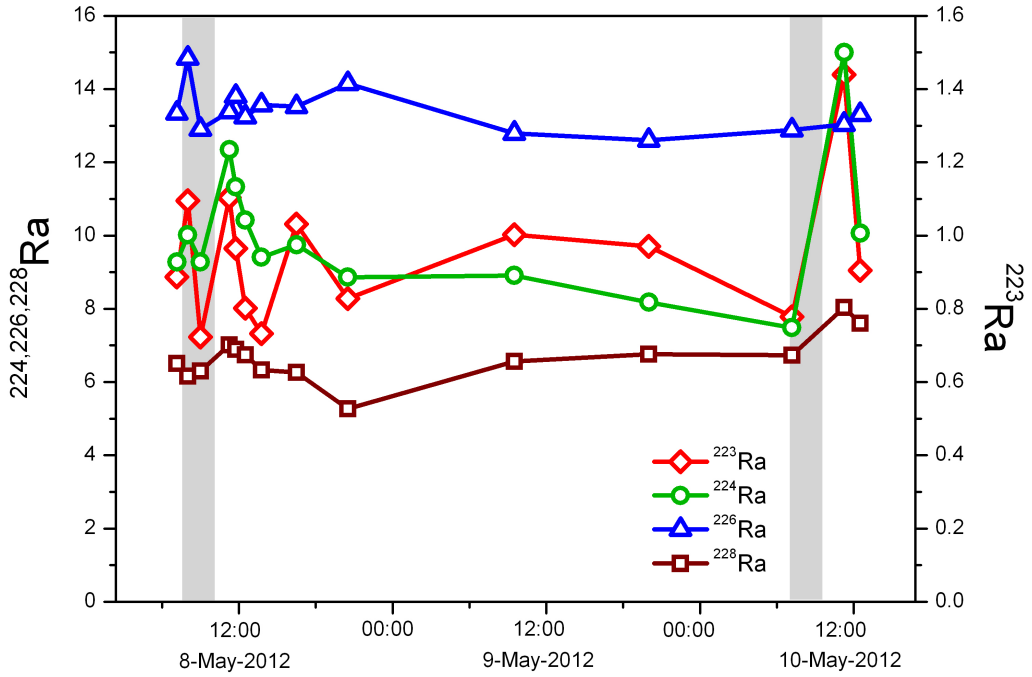

884

885 **FIGURE 7**

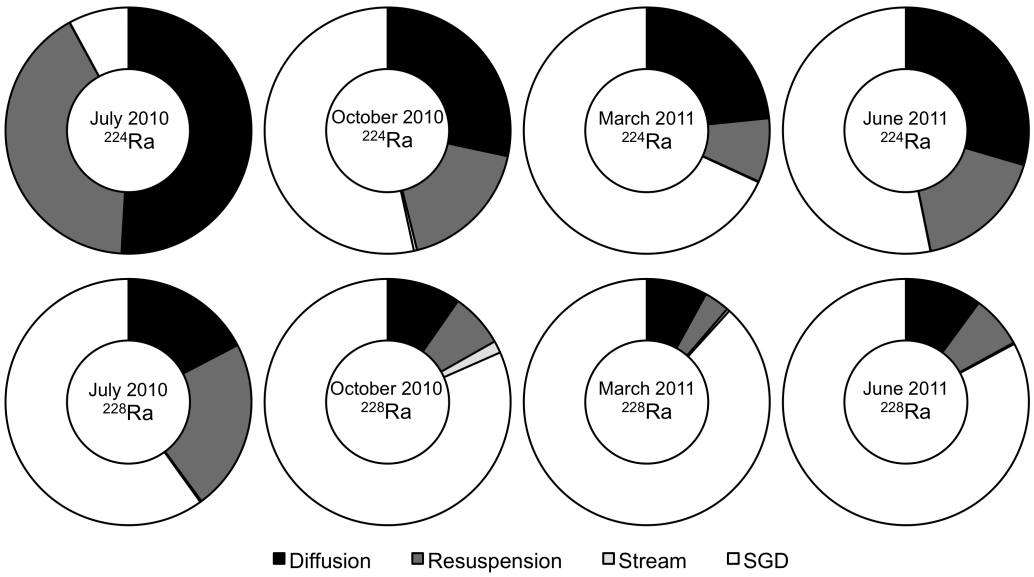

886